

# Inverse modelling for predicting both water and nitrate movement in a structured-clay soil (Red Ferrosol)

James M. Kirkham<sup>1</sup>, Christopher J. Smith<sup>2</sup>, Richard B. Doyle<sup>1</sup> and Philip H. Brown<sup>3</sup>

<sup>1</sup> Tasmanian Institute of Agriculture, University of Tasmania, Hobart, TAS, Australia

<sup>2</sup> Land and Water, CSIRO, Canberra, ACT, Australia

<sup>3</sup> Centre for Plant and Water Science, Central Queensland University, Bundaberg, QLD, Australia

## ABSTRACT

Soil physical parameter calculation by inverse modelling provides an indirect way of estimating the unsaturated hydraulic properties of soils. However many measurements are needed to provide sufficient data to determine unknown parameters. The objective of this research was to assess the use of unsaturated water flow and solute transport experiments, in horizontal packed soil columns, to estimate the parameters that govern water flow and solute transport. The derived parameters are then used to predict water infiltration and solute migration in a repacked soil wedge. Horizontal columns packed with Red Ferrosol were used in a nitrate diffusion experiment to estimate either three or six parameters of the van Genuchten–Mualem equation while keeping residual and saturated water content, and saturated hydraulic conductivity fixed to independently measured values. These parameters were calculated using the inverse optimisation routines in Hydrus 1D. Nitrate concentrations measured along the horizontal soil columns were used to independently determine the Langmuir adsorption isotherm. The soil hydraulic properties described by the van Genuchten–Mualem equation, and the  $\text{NO}_3^-$  adsorption isotherm, were then used to predict water and  $\text{NO}_3^-$  distributions from a point-source in two 3D flow scenarios. The use of horizontal columns of repacked soil and inverse modelling to quantify the soil water retention curve was found to be a simple and effective method for determining soil hydraulic properties of Red Ferrosols. These generated parameters supported subsequent testing of interactive flow and reactive transport processes under dynamic flow conditions.

**Subjects** Agricultural Science, Soil Science, Environmental Impacts

**Keywords** Pedotransfer functions, Water flow, Rosetta, Hydrus, Soil water, Nitrate, Hydrus-1D, Hydrus-2D

## INTRODUCTION

Simulation models are useful for examining water and solute movement in soil profiles, such as when improving water and nutrient use efficiency or designing fertigation systems (Cote *et al.*, 2003; Skaggs *et al.*, 2004; Siyal & Skaggs, 2009). There are a number of soil water models, such as LeachM (Wagenet & Hutson, 1989), Wet-Up (Cook *et al.*, 2003),

Submitted 30 March 2018  
Accepted 25 October 2018  
Published 16 January 2019

Corresponding author  
Richard B. Doyle,  
Richard.Doyle@utas.edu.au

Academic editor  
Samuel Abiven

Additional Information and  
Declarations can be found on  
page 19

DOI 10.7717/peerj.6002

© Copyright  
2019 Kirkham *et al.*

Distributed under  
Creative Commons CC-BY 4.0

**OPEN ACCESS**

Hydrus 1D ([Šimůnek et al., 2008](#)), Hydrus 2D/3D ([Šimůnek, Van Genuchten & Šejna, 2006](#)), and numerical procedures described by [Wu & Chieng \(1995a, 1995b\)](#) which are all capable of describing water flow, and in some cases solute transport, in one, two, or three dimensions. In this study, we selected the suite of Hydrus models, because they can simulate solute flow under both 1D and 3D conditions. The van Genuchten–Mualem water content, capillary pressure and hydraulic conductivity models were used to predict water flow ([Šimůnek, Van Genuchten & Šejna, 2006](#)), but physically realistic parameters are needed for the intended application if accurate predictions are to be made.

Inverse optimisation techniques have become increasingly popular for parameter estimation and many soil models now have user-friendly optimisation tools built in ([Hopmans et al., 2002](#); [Vrugt & Bouten, 2002](#); [Wöhling, Vrugt & Barkle, 2008](#); [Kandelous et al., 2011](#)). The method involves multiple calculations in which parameters are adjusted, using a method such as the Levenberg–Marquardt or Bayesian procedure, until predictions agree sufficiently well with the measured data ([Šimůnek, Van Genuchten & Šejna, 2006](#)). This has advantages over other techniques for estimating hydraulic parameters, such as pedotransfer functions (PTFs), because the optimised parameters are estimated directly from measured data for a particular soil hydrological problem of interest. Care however must be taken when using this method to ensure parameters are physically realistic and representative of the spatial scale of interest ([Hopmans et al., 2002](#); [Vrugt & Bouten, 2002](#); [Mallants et al., 2007](#); [Wöhling, Vrugt & Barkle, 2008](#)).

[Šimůnek et al. \(2000\)](#) used inverse optimisation to estimate soil hydraulic parameters from water content data measured in horizontal absorption columns. Similarly, inverse optimisation has been used in Hydrus to predict water flow from water potential and cumulative outflow data ([Van Dam, Stricker & Droogers, 1994](#); [Hopmans et al., 2002](#); [Arbat et al., 2008](#)). [Kandelous & Šimůnek \(2010a, 2010b\)](#) and [Kandelous et al. \(2011\)](#) used inverse optimisation to estimate soil hydraulic parameters to predict water distribution from a point source, including subsurface irrigation, in the field. [Mallants et al. \(2007\)](#) used Hydrus 2D and cumulative infiltration data from a deep borehole infiltration test in clayey gravel and carbonated loess soil to estimate field-scale soil hydraulic properties.

Despite the increasing popularity of inverse optimisation, there are few published examples in which parameters derived from unsaturated flow absorption columns have been tested in 3D flow scenarios. Obtaining parameters for a specific flow scenario does not guarantee they will be suitable for extrapolation outside the measured data set to which they were fitted ([Sonnleitner, Abbaspour & Schulin, 2003](#)). [Vrugt & Bouten \(2002\)](#) and [Wöhling, Vrugt & Barkle \(2008\)](#) recommend the use of the Metropolis algorithm to determine parameter uncertainty, given measurement errors and the models inability to perfectly represent the system. However, if the derived parameters can be shown to be capable of approximating the observed water content distribution under contrasting conditions, it is likely they are physically realistic for the conditions being investigated. To this end, [Sonnleitner, Abbaspour & Schulin \(2003\)](#) and [Kandelous et al. \(2011\)](#) used inverse parameter estimation to improve simulations of water content data under different flow scenarios. Minimising the number of optimised parameters, increases the likelihood that the parameters are physically realistic ([Hopmans et al., 2002](#)).

Although several numerical models, including Hydrus ([Hanson, Šimůnek & Hopmans, 2006](#)), have looked at reactive solute transport ([Molinero et al., 2008](#); [Kuntz & Grathwohl, 2009](#); [Nakagawa et al., 2010](#)), validation of the models has been limited. [Phillips \(2006\)](#) used Hydrus and some unpublished data to predict the transport of  $K^+$  in unsaturated repacked horizontal columns of reactive soil similar to the one used in this study. In field-scale simulations using Hydrus 1D, [Persicani \(1995\)](#) and [Moradi, Abbaspour & Afyuni \(2005\)](#) had limited success in simulating reactive metal movement over extended time-scales. However, [Rassam & Cook \(2002\)](#) were able to use modelling of solute fluxes in soils to explain results from the field and laboratory measurements of [Rassam, Cook & Gardner \(2002\)](#). Recently, [Ramos et al. \(2011, 2012\)](#) provide examples where Hydrus was successfully used to predict water and solute movement under saline conditions. Validation of the reactive solute module in Hydrus has received considerable attention; however a continued effort is needed to demonstrate its ability to properly investigate soil hydrological processes and reactive transport.

In this paper, we use inverse parameter estimation to determine soil hydraulic properties from measured water content profiles in horizontal soil columns (1D transport), and apply the parameters to predicting water flow from a point source into a wedge of soil. We also investigated  $NO_3^-$  transport, using an adsorption isotherm determined in the horizontal soil columns that were subsequently used in Hydrus 2D/3D to predict  $NO_3^-$  distributions in the soil wedge under two different irrigation scenarios.

## MATERIALS AND METHODS

Experiments used surface soil (0–15 cm) of a free-draining, well-structured Red, Mesotrophic, Humose, Ferrosol ([Isbell, 1996](#)). Soil was collected from Moina in northwest Tasmania, Australia (41°29'28.80"S and 14°60'34.70"E) from a site under long-term pasture. Samples of soil were air-dried at 40 °C, sieved to retain the <2 mm fraction and stored for later use. Chemical and physical properties are presented in [Table 1](#).

Soil pH and electrical conductivity (EC) were measured on 1:5 soil to water extracts ([Rayment & Higginson, 1992](#)). Solution concentrations were measured from soil samples wet to a water content of 0.55  $g_w g^{-1}$  soil. The solution was extracted by centrifuging samples with 10  $cm^3$  of 1,1,2-trichloro-1,2,2-trifluoroethane (TFE) as described by [Phillips & Bond \(1989\)](#). Exchangeable cations were determined by extraction with 1M  $NH_4Cl$  after the water-soluble ions had been extracted. Organic carbon was analysed using the [Walkley & Black \(1934\)](#) method. Particle size analysis (United States Department of Agriculture (USDA); [Gee & Bauder, 1986](#)) was undertaken by pipette method after pretreatment to remove both organic carbon and iron oxides (FeO) using hydrogen peroxide and sodium dithionite, respectively ([McKenzie, Coughlan & Cresswell, 2002](#)). Semiquantative mineralogy was determined using X-ray diffraction on the pretreated clay fraction from the particle size analysis.

### Horizontal solute absorption

Absorption of a  $NO_3^-$  solution by the soil was measured in horizontal columns between 17 and 50 cm in length depending on absorption periods. The air dry soil was moistened

**Table 1** Soil chemical and physical properties for the surface soil (0–15 cm depth).

pH	5.8					
EC (mS cm <sup>-1</sup> )	0.10					
Soil solution cations	Ca	K	Mg	Na	NH <sub>4</sub> -N	
(μmol <sub>c</sub> cm <sup>-3</sup> soil solution)	46.5	19.96	11.04	18.32	13.33	
Soil solution anions	NO <sub>3</sub> -N	Cl	PO <sub>4</sub> -P	SO <sub>4</sub> -S		
(μmol <sub>c</sub> cm <sup>-3</sup> soil solution)	45.84	15.07	0.52	2.90		
Exchangeable cations	Ca	K	Mg	Na		
(μmol <sub>c</sub> g <sup>-1</sup> soil)	827.46	114.17	83.34	0		
Organic carbon (%)	4.73					
Particle size distribution (%)	sand	silt	clay			
OC removed	80	12	8			
OC and iron oxides removed	45	22	33			
Clay mineralogy (%)	Quartz	amorphous	Kaolinite, organic	Garnet, Gibbsite	Epidote	Smectite, Rutile, Amphibole
	25–35	15–25	10–15	5–10	2–5	<5

before packing into the columns. Columns were packed (using a drop hammer) with relatively dry soil (water content 0.15 g g<sup>-1</sup>) in two to three g increments to achieve a bulk density of close to 1.03 g cm<sup>-3</sup>, which is similar to that measured in the field. Using a Mariotte bottle, a 110 μmol<sub>c</sub> cm<sup>-3</sup> NO<sub>3</sub><sup>-</sup> solution was applied to the inlet of the soil column at zero suction. The outlet of the column remained open, tamped with cotton wool to hold the soil in place. Flow was stopped at set times and the column divided into sections that ranged from 1 to 2.5 cm. Short sections were placed near the wetting front to provide an accurate measure of the solute and water contents in this area. The soil sections were transferred to tubes and weighed to determine moist weight.

Two types of column experiments were conducted, and are referred to as Set A and Set B. Each individual experiment in both Set A and Set B used a freshly prepared soil column. Set A consisted of five experiments with infiltration times of 26, 30, 43, 47, and 70 min. In these experiments, water-soluble NO<sub>3</sub><sup>-</sup> vs distance in the column was determined by adding deionised water to each column section to make a soil-to-water ratio of 1:5.5 (SD ± 0.4). The soil plus water was weighed. Samples were shaken for 4 h in an end-over-end shaker, centrifuged at 9,800 m s<sup>-2</sup> for 10 min, and the supernatant decanted and weighed. The soil remaining in the tubes was also weighed.

Set B involved four columns with absorption times for two of 80 and 320 min for the others. Duplicate columns in this series were either (i) extracted as in Set A or (ii) the soil solution was extracted using the TFE method described by [Phillips & Bond \(1989\)](#).

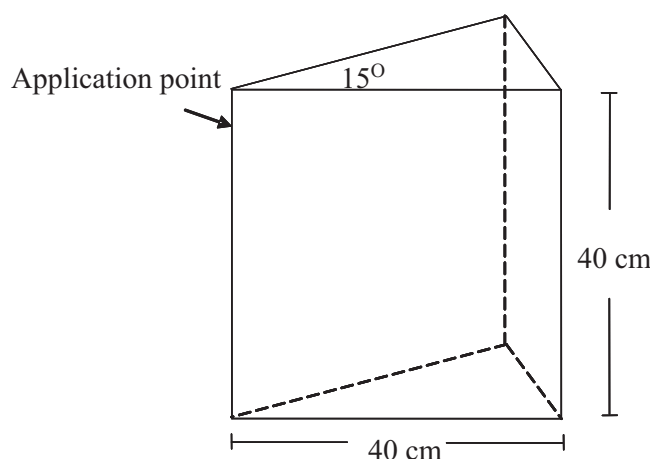


**Figure 1** Geometry of the wedge apparatus.

Full-size  DOI: 10.7717/peerj.6002/fig-1

The adsorbed  $\text{NO}_3^-$  was extracted by adding a volume of 2M KCl to form a 1:5.5 (SD  $\pm$  0.5) soil:solution ratio (Rayment & Higginson, 1992).

The tubes were reweighed and shaken for 1 h to extract adsorbed  $\text{NO}_3^-$ . The soil plus 2M KCl samples were centrifuged at  $9,800 \text{ m s}^{-2}$  for 10 min, and the supernatant decanted in preweighed falcon tubes and weighed. The soil remaining in the tubes was washed twice by shaking for 30 min in  $20 \text{ cm}^3$  deionised water to remove residual salts. The tubes were centrifuged at  $9,800 \text{ m s}^{-2}$  for 10 min and the wash solution discarded. The washed soil was oven-dried at  $105^\circ \text{C}$  and weighed to give the oven-dry mass of soil in each section. Water and KCl extracts were analysed for  $\text{NO}_3^-$ -N on an Alpchem autoanalyser (Alpkem, 1992).

## Point-source solute infiltration

Perspex wedges were constructed with the same dimensions described by Li, Zhang & Ren (2003) and packed with dry soil (water content of  $0.2 \text{ g g}^{-1}$ ) to a bulk density of  $0.95 \text{ g cm}^{-3}$ . All solutions were applied to the  $15^\circ$  corner of the wedge at a depth of five cm (Fig. 1) with a peristaltic pump set to deliver solution at  $50 \text{ cm}^3 \text{ h}^{-1}$ , equivalent to a dripper output of  $1,200 \text{ cm}^3 \text{ h}^{-1}$  in a  $360^\circ$  flow environment.

Figure 2 shows the two irrigation scenarios applied to the wedge experiments. Both treatments were irrigated for 0.5 h (equivalent to  $25 \text{ cm}^3$  of solution) with the  $\text{NO}_3^-$  solution applied to the horizontal columns, that is  $110 \mu\text{mol}_e \text{ NO}_3^- \text{ cm}^{-3}$ . This was immediately followed by a 1.5 h application of solute free water ( $75 \text{ cm}^3$ ). The soil was either (i) sampled immediately after the water application (Scenario A) or (ii) allowed to rest for 16 h before irrigating again with water for 6 h ( $300 \text{ cm}^3$ ) prior to sampling (Scenario B). That is, a total of  $375 \text{ cm}^3$  of water was applied to the wedge in Scenario B with samples being taken 24 h after initial application of the solute. A single replicate was used for Scenario A and Scenario B was duplicated.

Soil was sampled using the method described by Li, Zhang & Ren (2003). Briefly, a five cm grid was placed over the column and a soil core (two cm internal diameter) taken from the centre of each grid. Additional soil samples were taken at the edge of the wetting front. The soil from the core was sub-sampled to determine gravimetric water content

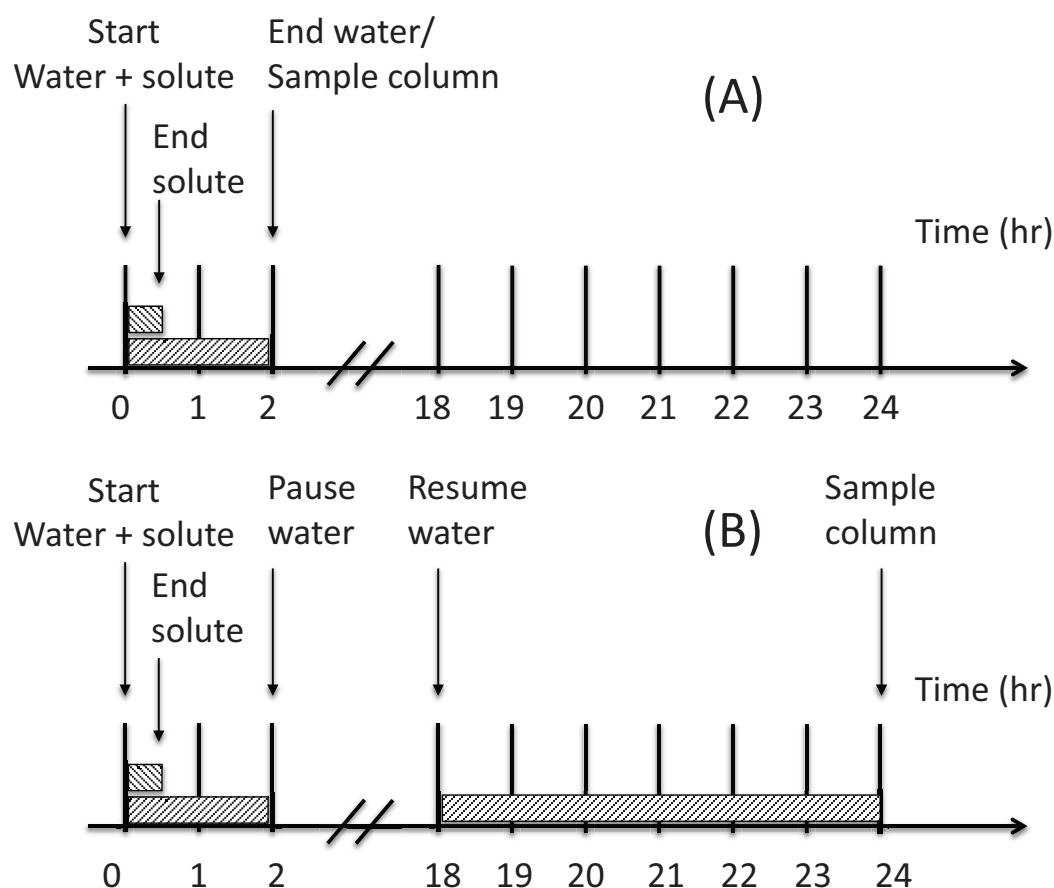


**Figure 2** Schematic of the two irrigation scenarios (A) and (B) applied to the wedge columns.

Full-size [DOI: 10.7717/peerj.6002/fig-2](https://doi.org/10.7717/peerj.6002/fig-2)

and total  $\text{NO}_3^-$  concentration (solution and adsorbed). Wet soil was extracted with 2M KCl (1:10 soil: KCl ratio) and analysed on an Alpchem autoanalyser (Rayment & Higginson, 1992). Calculations of total  $\text{NO}_3^-$  partitioned into the solution and the amount of adsorbed  $\text{NO}_3^-$  were done using the adsorption isotherm determined from the horizontal column data (described below).

### Nitrate adsorption isotherm

Partitioning of  $\text{NO}_3^-$  between the adsorbed and solution phases, over the range of soil solution concentrations in the columns, was measured by displacing the soil solution with TFE (Phillips & Bond, 1989). The Langmuir equation (Eq. (1)) was then fitted to the data to describe the  $\text{NO}_3^-$  adsorption isotherm.

$$C_a = \frac{C_{\max} \phi C_w}{1 + \phi C_w}, \quad (1)$$

where  $C_a$  is the concentration of adsorbed solute ( $\mu\text{mol}_c \text{ g}^{-1}$ ),  $C_w$  is the concentration of solute in the soil solution ( $\mu\text{mol}_c \text{ cm}^{-3}$ ),  $C_{\max}$  is the maximum amount of solute that can be adsorbed by the soil ( $\text{g cm}^{-3}$ ), and  $\phi$  determines the magnitude of the initial slope of the isotherm (Sposito, 1989).

$C_{\max}$  and  $\phi$  were determined using the Gauss–Newton nonlinear curve model in the statistical program SAS (version 9.1; SAS, Cary, NC, USA).  $C_{\max}$  and  $\phi$  were determined to be 23.17 (95% confidence interval (CI)  $\pm 3.43$ ) and 0.00766 (95% CI  $\pm 0.00194$ ), respectively.

## Hydrus flow equations

Water flow is described by the Richards equation modified to describe horizontal flow in one dimension with no loss of water due to evaporation of root uptake (*Šimůnek et al., 2008*):

$$\frac{\partial \theta}{\partial t} = \frac{\partial}{\partial x} \left( K \frac{\partial \psi}{\partial x} \right),$$

where  $\theta$  is the volumetric water content ( $\text{cm}^3 \text{ cm}^{-3}$ ),  $t$  is time (min),  $x$  is the horizontal distance (cm),  $\psi$  is the water tension (cm), and  $K$  is the hydraulic conductivity ( $\text{cm min}^{-1}$ ) given by:

$$K(\psi, x) = K_{\text{sat}}(x) K_r(h, x),$$

where  $K_r$  is the relative hydraulic conductivity (no unit) and  $K_{\text{sat}}$  is the saturated hydraulic conductivity ( $\text{cm min}^{-1}$ ; *Šimůnek et al., 2008*).

The modified form of the Richards equation that describes water movement in two dimensions assuming no loss of water through root uptake or evaporation can be written (*Šimůnek, Van Genuchten & Šejna, 2006*):

$$\frac{\partial \theta}{\partial t} = \frac{\partial}{\partial x_i} \left[ K \left( K_{ij}^A \frac{\partial \psi}{\partial x_j} \right) + K_{iz}^A \right]$$

where  $x_i$  ( $i = 1, 2$ ) are the spatial coordinates (cm), and  $K_{ij}^A$  and  $K_{iz}^A$  are components of a dimensionless anisotropy tensor  $K^A$ . Assuming flow is isotropic (i.e.  $K$  is equal in horizontal and vertical directions) the diagonal entries of  $K_{ij}^A$  equal one and the off-diagonal entries equal zero (*Šimůnek, Van Genuchten & Šejna, 2006*).

In the two-dimensional flow scenario  $K$  is given by:

$$K(\psi, x) = K_{\text{sat}}(x, z) K_r(h, x, z).$$

If the modified form of the Richards equation is applied to planar flow in a vertical cross section,  $x_1 = x$  is the horizontal coordinate and  $x_2 = z$  is the vertical coordinate. This equation can also describe axisymmetric flow when  $x_1 = x$  represents a radial coordinate (*Gardenas et al., 2005*). The transcripts  $i$  and  $j$  denote either the  $x$  or  $z$  coordinate.

To solve the Richards equation, Hydrus implements the soil hydraulic functions of the van Genuchten–Mualem to describe unsaturated hydraulic conductivity in terms of soil water retention parameters (*Šimůnek, Van Genuchten & Šejna, 2006*). Water retention is described by *Šimůnek, Van Genuchten & Šejna (2006)* as:

$$\theta(\psi) = \begin{cases} \theta_r \frac{\theta_s - \theta_r}{[1 + |\alpha\psi|^n]^m} & \psi < 0 \\ \theta_s & \psi \geq 0 \end{cases}$$



and unsaturated conductivity is written (*Šimůnek, Van Genuchten & Šejna, 2006*):

$$K(\psi) = K_s S_e^l \left[ 1 - (1 - S_e^{1/m})^m \right]^2 \quad \psi < 0$$

where:

$$m = 1 - 1/n, \quad n > 1$$

and:

$$S_e = \frac{\theta - \theta_r}{\theta_s - \theta_r}$$

In the above equations  $\theta_r$  is the residual water content ( $\text{cm}^3 \text{cm}^{-3}$ ),  $\theta_s$  is the saturated water content ( $\text{cm}^3 \text{cm}^{-3}$ ),  $\alpha$  ( $\text{cm}^{-1}$ ),  $n$  (no unit), and  $l$  (no unit) are curve fitting parameters for the hydraulic conductivity function and  $S_e$  is the effective water content ( $\text{cm}^3 \text{cm}^{-3}$ ).

When the van Genuchten–Mualem model is used to solve Richards equation in Hydrus there are six soil hydraulic parameters required ( $\theta_r$ ,  $\theta_s$ ,  $\alpha$ ,  $n$ ,  $l$ , and  $K_{\text{sat}}$ ).

The Langmuir equation was used to predict the reactive solute transport. In Hydrus, desorption of a nontransforming solute is described by the generalised nonlinear equation (*Šimůnek, Van Genuchten & Šejna, 2006*):

$$C_a = \frac{k_s C_w^\omega}{1 + \phi C_w^\omega}, \quad (2)$$

and:

$$\frac{\partial C_a}{\partial t} = \frac{k_s \omega C_w^{\omega-1}}{(1 + \phi C_w^\omega)^2} \frac{\partial C_w}{\partial t} + \frac{C_w^\omega}{1 + \phi C_w^\omega} \frac{\partial k_s}{\partial t} - \frac{k_s C_w^{2\omega}}{(1 + \phi C_w^\omega)^2} \frac{\partial \phi}{\partial t} + \frac{k_s C_w^\omega \ln C_w}{(1 + \phi C_w^\omega)^2} \frac{\partial \omega}{\partial t}, \quad (3)$$

where  $k_s$  ( $\text{cm}^3 \text{g}^{-1}$ ),  $\omega$  (dimensionless), and  $\phi$  ( $\text{cm}^3 \text{g}^{-1}$ ) are constants. In the case of the Langmuir equation,  $k_s = C_{\text{max}} \phi$  (where  $C_{\text{max}}$  and  $\phi$  are the Langmuir equation constants from Eq. (1)) and  $\omega = 1$ .

## Estimation of flow equations parameters

Soil hydraulic parameters for the van Genuchten equation were determined using the inverse optimisation procedure in Hydrus 1D (*Šimůnek et al., 2008*). Water profile data from the soil columns in Set A were used, after removing obvious outliers in the data that were determined to be due to soil loss during column sampling (*Hopmans et al., 2002*). The initial water content was set to  $0.15 \text{ cm}^3 \text{cm}^{-3}$ , the measured water content of the repacked columns, for all optimisations. Free water absorption was simulated by applying constant water content boundary condition of  $0.64 \text{ cm}^3 \text{cm}^{-3}$  to the opening of the column. The lower boundary condition was set to free drainage. The maximum number of iterations was set to 50 and 86 water content points across five time steps were used in the inverse scenario from the Set A column experiments. Weighting of inverse data was by standard deviation and an equal weighting was applied to all the water content values. Residual soil water content ( $\theta_r$ ),  $\theta_s$ , and  $K_{\text{sat}}$  were set or optimised depending on the optimisation scenario (*Fit All* is the term applied when all parameters were optimised and *Set Measured* is used when  $\theta_r$ ,  $\theta_s$ , and  $K_{\text{sat}}$  were set to independently measured values).



The remaining empirical parameters,  $\alpha$ ,  $n$ , and  $l$  were fitted by running the inverse parameter estimation option in Hydrus 1D. The initial values of  $\alpha$ ,  $n$ , and  $l$  were based on the default values given for the Loam soil in Hydrus 1D ( $\alpha = 1.56$ ,  $n = 0.173$ , and  $l = 0.5$ ).

Initial estimates for  $\theta_r$  and  $\theta_s$  were 0.05 and 0.58 ( $\text{cm}^3 \text{cm}^{-3}$ ) and  $K_{\text{sat}}$  was set to  $0.10 \text{ cm min}^{-1}$ . Saturated soil water content ( $\theta_s$ ) and  $K_{\text{sat}}$  values were independently measured in falling head  $K_{\text{sat}}$  experiments (Reynolds et al., 2002). A column of water (4.2 cm in diameter and 12 cm high) was applied to wet repacked soil core packed to a bulk density of 1.0 with air dry soil sieved to <2 mm. The soil cores were two cm high and had an internal diameter the same as the water column sitting above it. Triplicate measurements of conductivity were recorded on four separate cores. Residual soil water content ( $\theta_r$ ) was estimated based on the air-dry soil water content.

The Rosetta PTF model (Schaap, Leij & Van Genuchten, 2001) was used to estimate soil hydraulic properties as a comparison against the inverse modelling method. The soil particle size measurements (Table 1) and bulk density ( $1.03 \text{ g cm}^{-3}$ ) were used to estimate soil hydraulic parameters. In a second prediction, moisture retention at  $-33$  and  $-1,500 \text{ kPa}$  ( $0.34$  and  $0.22 \text{ cm}^3 \text{cm}^{-3}$ , respectively) were also included as inputs into Rosetta. The water content at  $-33 \text{ kPa}$  was determined on a suction table apparatus and  $-1,500 \text{ kPa}$  were determined using pressure plate apparatus (Cresswell, 2002).

### Modelling water and solute absorption in soil wedges

Hydrus 2D/3D was used to model water distribution in the horizontal column experiments based on the same initial and boundary conditions used in Hydrus 1D during inverse optimisation. Horizontal flow in Hydrus 2D/3D was simulated by setting the geometry to a 2D horizontal plane. The geometry of the flow domain was set to a column two cm in diameter and 50 cm long. Soil hydraulic parameters having the lowest values for the objective function were used to simulate water absorption. Nitrate absorption was predicted by applying a third-type (Cauchy) solute boundary at the inlet of the column ( $x = 0 \text{ cm}$ ) at a constant concentration of  $110 \mu\text{mol NO}_3^- \text{cm}^{-3}$ . Bulk density was set to the measured value of  $1.03 \text{ g cm}^{-3}$ , longitudinal and transverse dispersivities were set to 0.3 and 0.03 cm, respectively (Ajdary et al., 2007), and the diffusion coefficient was neglected as it was considered negligible relative to the dispersion (Hanson, Šimůnek & Hopmans, 2006; Ajdary et al., 2007). Parameters for the Langmuir equation (Eq. (1)) to describe  $\text{NO}_3^-$  adsorption were determined from the data measured in column Set B.

### Modelling water and solute in horizontal columns

To simulate water and  $\text{NO}_3^-$  distribution in the wedge experiments, a  $40 \times 40 \text{ cm}$  flow domain was created in a 2D axisymmetrical vertical flow geometry. The infiltration point at five cm depth was represented by a semicircle with three cm radius. The flux from the source was  $10.61 \text{ cm h}^{-1}$  (Eq. (4)), equivalent to a dripper output of  $1,200 \text{ cm}^3 \text{h}^{-1}$ .

$$\sigma = \frac{Q}{4 \pi r^2}, \quad (4)$$

**Table 2** Parameter estimation results for the *Fit All* and *Set Measured* parameter sets.

Inverse scenario	$\theta_r$ (cm <sup>3</sup> cm <sup>-3</sup> )	$\theta_s$ (cm <sup>3</sup> cm <sup>-3</sup> )	$\alpha$ (cm <sup>-1</sup> )	$n$	$K_{sat}$ (LT <sup>-1</sup> )	$l$	$\Phi$
<i>Fit All</i>	0.112 (0.247)	0.560 (0.007)	0.036 (0.006)	2.030 (0.684)	0.115 (0.061)	3.847 (5.442)	0.014
<i>Set Measured</i>	0.054 (0.003*)	0.580 (0.04*)	0.038 (0.005)	2.335 (0.279)	0.104 (0.029*)	3.175 (0.578)	0.020

**Notes:**

Values in parentheses show the 95% confidence intervals of the estimated parameters.  $\Phi$  indicates the value of the objective function.

\* Independently measured.

where  $\sigma$  is the flux from the surface of the source (cm h<sup>-1</sup>),  $Q$  is the total volumetric flux (cm<sup>3</sup> h<sup>-1</sup>), and  $r$  is the radius of the spherical source (cm).

The finite element mesh of the flow domain, which determines the level of model resolution in the calculations, was set to 0.5 cm in both  $z$  and  $h$  directions. No flux was allowed through the column boundaries. The infiltration source was set as a variable flux boundary so that water and solute applications could be controlled according to the two irrigation scenarios described for the wedge columns (Fig. 2). Nitrate absorption was predicted in the same way as for the horizontal columns. The time-variable boundary condition was used to apply the solute (110  $\mu\text{mol}_c \text{NO}_3^- \text{cm}^{-3}$ ) only for the first 0.5 h of water application to the column.

## Statistical analysis

The root mean square error (RMSE) was calculated as the error between the measured and simulated water content and  $\text{NO}_3^-$  concentrations. Comparisons of the RMSE values with predictions from different parameter sets allowed those that produced the lowest errors to be identified. Comparisons of simulated RMSE values with those calculated from measured data allowed the significance of the model error to be assessed in relation to measurement error. This method has been commonly used to measure the quality of model predictions in previous studies (Skaggs *et al.*, 2004; Ajdary *et al.*, 2007; Arbat *et al.*, 2008; Patel & Rajput, 2008). Part of the inverse modelling in Hydrus 1D allows calculation of a correlation matrix that specifies the correlation between the fitted coefficients and statistical information about the fitted parameters.

## RESULTS

### Parameter determination and model validation in horizontal columns

Values for soil hydraulic parameters estimated from column Set A are presented in Table 2. The two inverse scenarios produced slightly differing values, with the *Fit All* parameters having a lower value for the objective function  $\Phi$  than the *Set Measured* suggesting that the former gave a slightly closer fit between the predicted and measured soil water profiles. The 95% CIs for the optimised values for  $\alpha$ ,  $n$ , and  $l$  were smaller compared to the values when all parameters were optimised. The parameters in the *Fit All* scenario had higher uncertainty and greater correlation between fitted parameters compared to the *Set Measured* parameters (Tables 2 and 3). The correlation matrix shows there were three high values in the *Fit All* parameter function compared to one in the *Set Measured* results;  $\alpha$  and  $n$  being highly correlated (Table 3, bold entries). High correlation values

**Table 3** Correlation matrix of the inverse function.

<i>Fit All</i>	$\theta_r$	$\theta_s$	$\alpha$	$n$	$K_{sat}$	$l$
$\theta_r$	1.000					
$\theta_s$	0.016	1.000				
$\alpha$	<b>0.977</b>	−0.046	1.000			
$n$	0.656	−0.243	0.561	1.000		
$K_{sat}$	−0.753	0.118	−0.649	<b>−0.976</b>	1.000	
$l$	<b>−0.975</b>	−0.149	−0.941	−0.605	0.737	1.000
<i>Set Measured</i>	$\alpha$	$n$	$l$			
$\alpha$	1.000					
$n$	<b>0.937</b>	1.000				
$l$	−0.283	0.063	1.000			

(magnitude >0.9) indicate parameter nonuniqueness and a correspondingly high uncertainty (Hopmans *et al.*, 2002; Šimůnek & Van Genuchten, 1996). The optimised value of  $\theta_r$  was 0.112 and the 95% CI that ranged from −0.135 to 0.359, which includes the measured value ( $0.054 \pm 0.003$ ). Saturated water content ( $\theta_s$ ) was 0.56 (0.553–0.567) and was significantly different from the independently measured values ( $0.58 \pm 0.04$ ; Table 2). The measured  $K_{sat}$  ( $0.104 \pm 0.0299$ ) fall within the 95% CI [0.054–0.176; mean best fit value of 0.115] of the optimised value.

The two parameter sets were tested against independently measured data from the horizontal columns (Column data Set B) and the point-source wedge experiments. Predicted water distributions and measured water content in the horizontal columns from column Set B are shown in Fig. 3A. We have plotted  $\theta$  and  $\text{NO}_3^-$  profiles against the Boltzmann variable  $X$  (distance/ $\sqrt{\text{time}}$ ;  $\text{cm s}^{-1/2}$ ; Smiles *et al.*, 1978; Phillips & Bond, 1989). Both parameter sets showed similarly good correspondence to the measured data (continuous and dotted lines), which is confirmed by the RMSE and  $R^2$  values (Table 4). Accurate predictions of  $\theta$  profiles after absorbing water for 80 and 320 min are not surprising given that data from Set A (27–70 min) are not statistically different from Set B when normalised against the Boltzmann variable. The results, however, do show that under the unsaturated absorption scenario, predictions made for longer times (80 and 320 min) are still accurate when the predictions are extended beyond the range of optimised data. The consistency between predictions based on short time  $\theta$  and  $\text{NO}_3^-$  data (Set A) and longer time  $\theta$  and  $\text{NO}_3^-$  data (Set B) further demonstrate the experiments had a good degree of repeatability and produced consistent data across a range of time scales.

In comparison, predicted water content using soil hydraulic parameters determined by Rosetta are shown in Fig. 4. These data show the piston front to be significantly behind the measured data (combined data from column Set A and B) especially when the water content at −33 and −1,500 kPa are included in the model. Removal of the FeO before determining the sand, silt, and clay content did not improve the predictions of water retention parameters or saturated hydraulic conductivity. Deriving the water retention

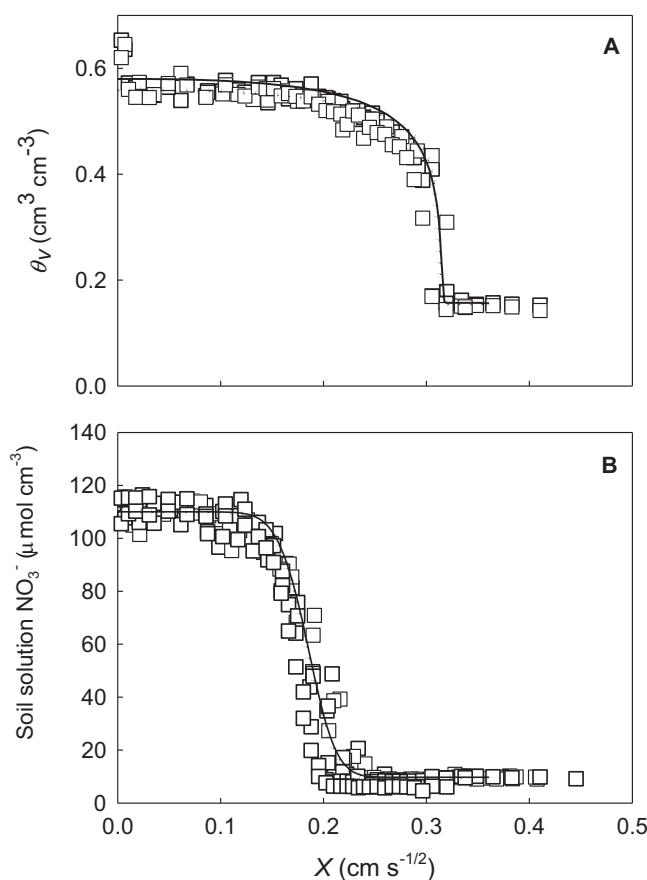


**Figure 3** (A) Fits of the *Fit All* (solid line) and *Set Measured* (dotted line) parameters to the measured water profile data (squares) from column Set B not included in the inverse optimisation. (B) Fits for soil solution  $\text{NO}_3^-$ .

[Full-size](#) DOI: 10.7717/peerj.6002/fig-3

**Table 4** Root mean square error (RMSE) of water and  $\text{NO}_3^-$  profiles determined using the *Fit All* and *Set Measured* parameters in comparison to the measured data in the horizontal column experiments presented in Fig. 3.

Inverse scenario	$\theta_v$ ( $\text{cm}^3 \text{cm}^{-3}$ )		$\text{NO}_3^-$ ( $\mu\text{mol}_e \text{cm}^{-3} \text{soln}$ )	
	RMSE	$R^2$	RMSE	$R^2$
<i>Fit All</i>	0.04	0.89	7.50	0.97
<i>Set Measured</i>	0.05	0.91	7.96	0.97
Measured <sup>†</sup>	0.04		6.19	

**Note:**

<sup>†</sup> “Measured” indicates the variation in the measured data calculated from the second set of horizontal soil columns where two  $\text{NO}_3^-$  and water measurements were made at identical points and times.

parameters and saturated hydraulic conductivity with Rosetta, values that use PTFs to predict the Van Genuchten parameters, produced significant inaccuracies in the predictions (see Fig. 4). In these experiments they are certainly less accurate than parameters derive from inverse modelling (Fig. 3).

The predicted  $\text{NO}_3^-$  distribution is shown in Fig. 3B. The measured and predicted  $\text{NO}_3^-$  distributions were compared from both Set A (27–70 min) and Set B

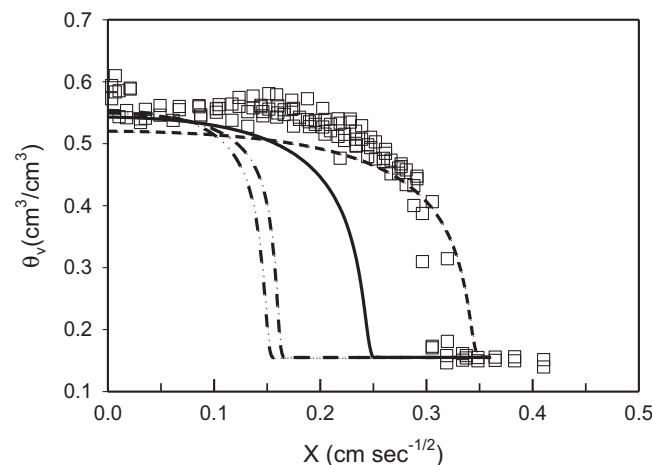


**Figure 4** Predicted volumetric water content using Rosetta derived soil hydraulic parameters and measured water profile data (squares) against the Boltzmann variable ( $X$ ). The *solid* line represents derived parameters using particle size data measured after removal of iron oxides and no water content data; the *dash* line represents parameters predicted using particle size without removing iron oxides and without water content data; the *dash-dot-dash* line refers to parameter predicted using particle size without removing iron oxides and with soil water content at  $-33$  and  $-1,500$  kPa; the *dash-dot-dot-dash* line refers to parameters predicted using particle size after removing iron oxides and with soil water content at  $-33$  and  $-1,500$  kPa.

Full-size [DOI: 10.7717/peerj.6002/fig-4](https://doi.org/10.7717/peerj.6002/fig-4)

(80 and 320 min) because the  $\text{NO}_3^-$  distribution was not used in the inverse optimisation. The good prediction of  $\text{NO}_3^-$  distribution by the two parameter sets, when the Langmuir isotherm parameters were included in the simulations, is confirmed by the  $R^2$  and RMSE values (Table 4). Due to the inaccuracy of water content prediction using Rosetta, no  $\text{NO}_3^-$  data are presented.

### Model validation using 3D wedge infiltration

The predicted distributions of water and  $\text{NO}_3^-$  throughout the soil wedge after the two irrigation scenarios are shown in Fig. 5. This figure also shows the positions of horizontal and vertical transects presented in Figs. 6 and 7. These figures show the agreement between the measured and predicted water and  $\text{NO}_3^-$  profiles in the wedge. Comparisons of the RMSE and  $R^2$  calculations indicated that both the *Fit All* and *Set Measured* parameter sets predicted very similar distributions, although the *Fit All* parameters produced slightly better predictions of  $\text{NO}_3^-$  distribution in the longer irrigation scenario. The measured RMSE, calculated from columns where duplicate measurements were taken at identical times and locations, were similar to the RMSE of the predicted values (Table 5). This indicates that the errors between the measured and predicted values were very similar to the errors of replicate measurements at identical points and times in the wedge experiments. The predictions achieved using the two parameter sets were therefore considered to be suitable to estimate water and  $\text{NO}_3^-$  distribution in the point-source flow scenario of the wedge column. The “*Set Measured*” parameters are preferred because there is less auto correlation between the fitted parameters ( $\alpha$ ,  $n$ ,  $l$ ).

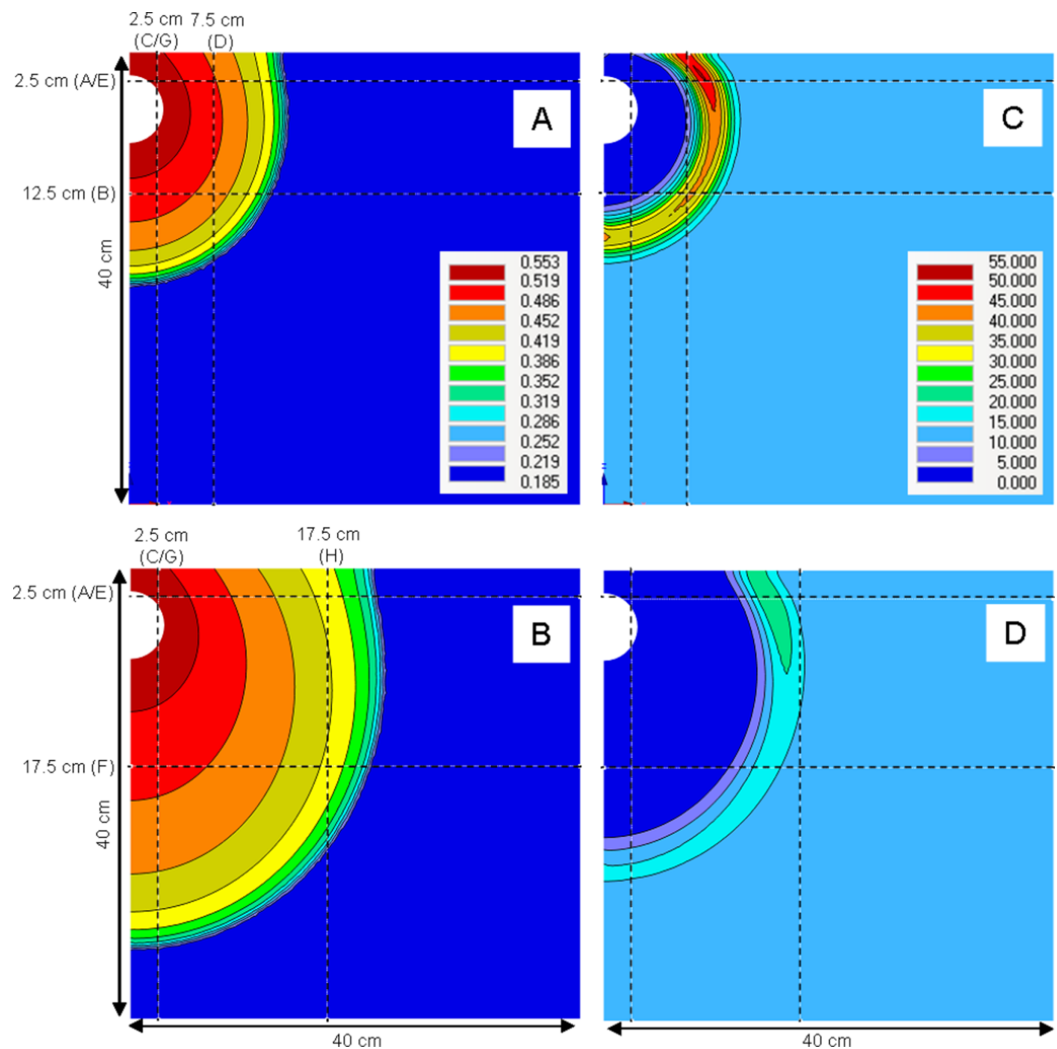


**Figure 5** Estimation of water and  $\text{NO}_3^-$  in the wedge experiment scenario using the *Set Measured* parameters. (A) and (C) show water content ( $\text{cm}^3 \text{cm}^{-3}$ ) and  $\text{NO}_3^-$  ( $\mu\text{mol cm}^{-3}$ ), respectively, for irrigation scenario A (2 h experiment, Fig. 2). (B) and (D) show water content ( $\text{cm}^3 \text{cm}^{-3}$ ) and  $\text{NO}_3^-$  ( $\mu\text{mol cm}^{-3}$ ), respectively, for irrigation scenario B (24 h experiment, Fig. 2). Horizontal and vertical transects and their symbols correspond to the water and solute profile plots in Figs. 6 and 7.

Full-size DOI: [10.7717/peerj.6002/fig-5](https://doi.org/10.7717/peerj.6002/fig-5)

## DISCUSSION

Inverse optimisation using Hydrus-1D can be used to effectively estimate soil hydraulic properties from simple 1D flow experiments. The flow parameters derived from 1D columns were suitable for describing flow under more complex 3D flow scenarios. These results show that the use of absorption columns offers an alternative to PTF methods and has the advantage that the parameters are determined using data from the actual soil type under consideration.

Comparisons of optimised parameters with independently measured data in the horizontal column showed that the fitted parameters were able to accurately predict water distribution in these flow scenarios. Further, water distribution could be accurately

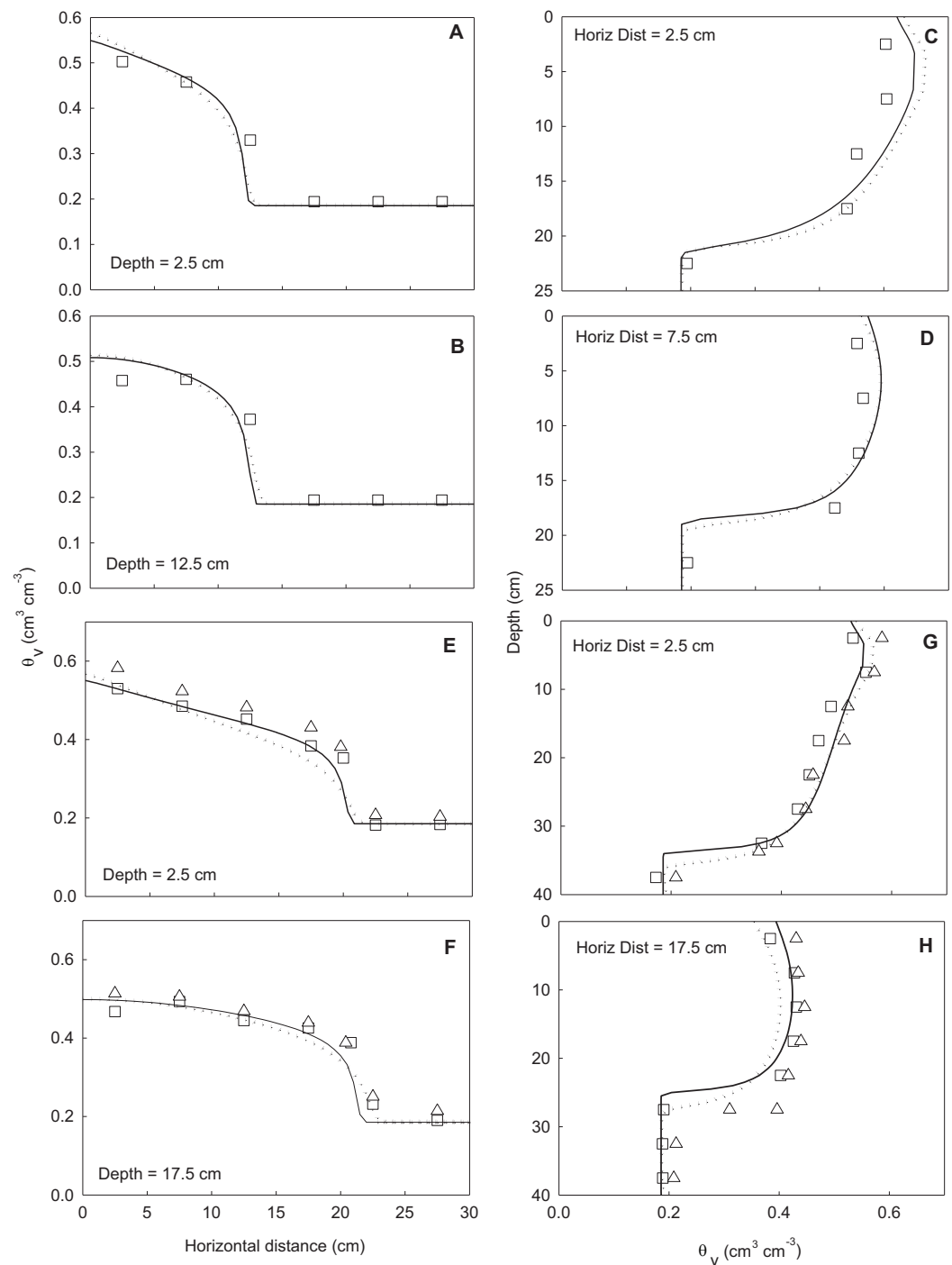


**Figure 6** Horizontal (A, B, E, F) and vertical transects (C, D, G, H) of water content ( $\text{cm}^3 \text{cm}^{-3}$ ) in the wedge columns. The symbols indicate measured data (squares represent replicate one and triangles replicate two). Solid lines represent simulations using the Fit All parameters and the dotted lines simulations using the Set Measured parameters. A to D show transects from irrigation scenario A (2 h experiment, Fig. 2) and E to H show transects from irrigation scenario B (24 h experiment, Fig. 2). Location of transects is shown in Fig. 5. The profiles were taken at same times as snapshots shown in Fig. 5.

Full-size [DOI: 10.7717/peerj.6002/fig-6](https://doi.org/10.7717/peerj.6002/fig-6)



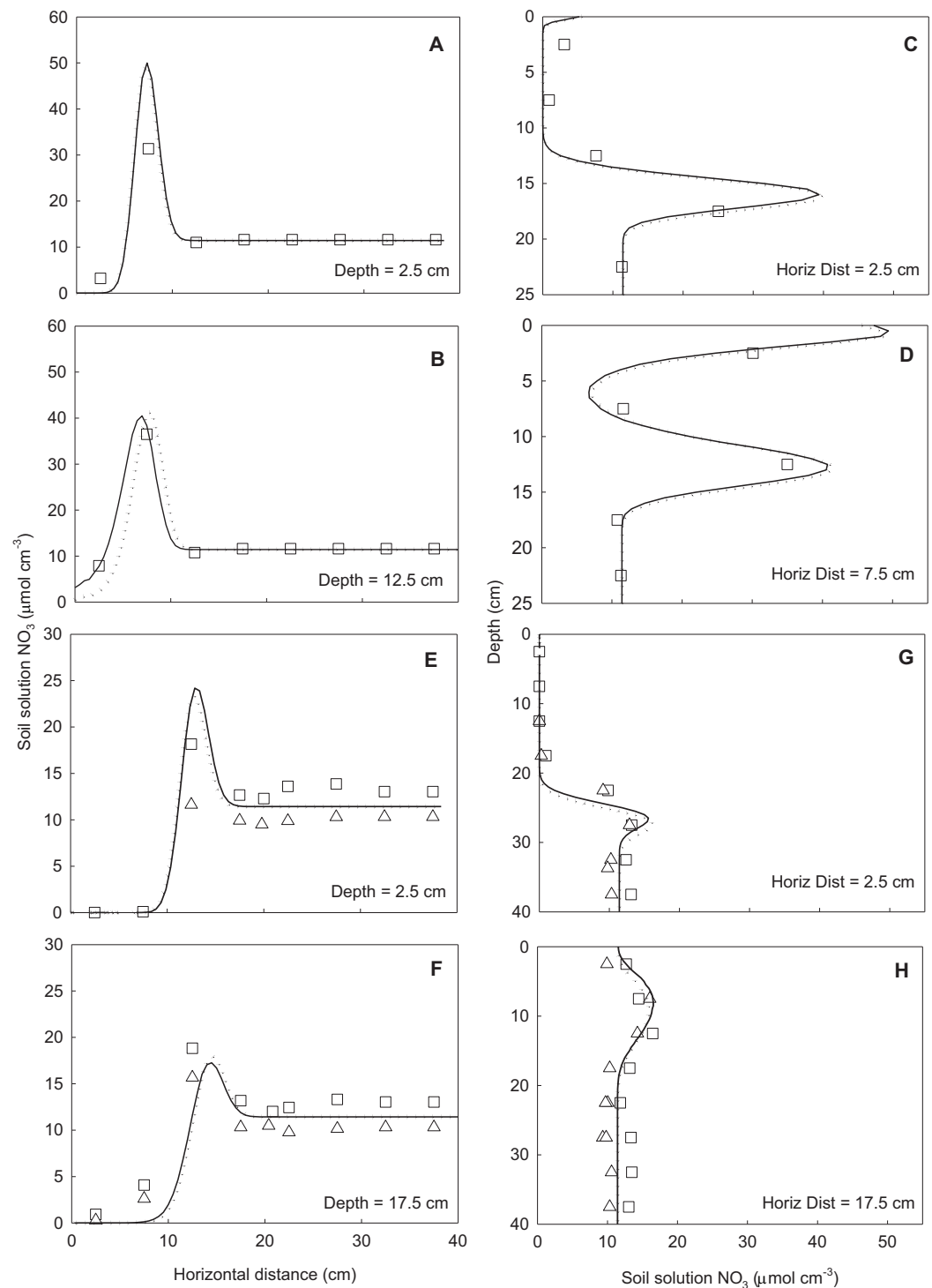


**Figure 7** Horizontal (A, B, E, F) and vertical (C, D, G, H) transects of soil solution  $\text{NO}_3^-$  concentration ( $\mu\text{mol cm}^{-3}$ ) in the wedge columns. Symbols indicate measured data (squares represent replicate one and triangles replicate two). Solid lines represent simulations using the *Fit All* parameters and dotted lines simulations using the *Set Measured* parameters. The  $\text{NO}_3^-$  reaction parameters were included in all simulations. Key to panels and transects same as for Fig. 5. The profiles were taken at same times as snapshots shown in Fig. 5.

Full-size DOI: 10.7717/peerj.6002/fig-7

**Table 5** Root mean square error (RMSE) of the fit of the two parameter sets used to predict water and  $\text{NO}_3^-$  distribution in the wedge experiments.

Parameters	Irrigation treatment	$\theta_v$ ( $\text{cm}^3 \text{ cm}^{-3}$ )		$\text{NO}_3^-$ ( $\mu\text{mol}_e \text{ cm}^{-3}$ solution)	
		RMSE	$R^2$	RMSE	$R^2$
<i>Fit All</i>	Scenario A	0.04	0.94	2.40	0.95
	Scenario B	0.03	0.97	3.05	0.81
<i>Set Measured</i>	Scenario A	0.04	0.96	2.16	0.95
	Scenario B	0.02	0.98	3.43	0.76
Measured <sup>†</sup>		0.03		2.64	

**Note:**

<sup>†</sup> “Measured” RMSE values indicate the variation in the measured data calculated from the wedge experiments from Irrigation Scenario B columns where two  $\text{NO}_3^-$  and water measurements were made at identical points in the wedges.

predicted for absorption periods four times longer than the data used in the inverse optimisation. This provides preliminary evidence that the parameters can predict water distribution outside the range of fitted values. However, this result is not surprising because the measured water content profiles coalesce to a single curve when presented against the Boltzmann variable  $X$  ( $\text{cm s}^{-1/2}$ ). Further evidence for this was provided by testing the parameters in the alternative point-source 3D flow scenario. The results presented in this paper demonstrate there is scope to use soil hydraulic parameters obtained from simple horizontal absorption experiments to accurately estimate water flow under more complex 3D conditions in uniform repack soil conditions (isotropic).

The inverse optimisations in this study produced two parameter sets that were capable of providing good predictions of water flow in the two flow scenarios. [Hopmans et al., \(2002\)](#) suggests that if various parameter sets produce similar model outcomes, the soil hydraulic parameters may be unidentifiable and the inverse optimisation may be ill-posed. However, our data ([Table 2](#)) shows that the values identified in the two scenarios are within the 95% CI estimates of the predictions; the difference between the parameter sets are therefore not significant. Limiting the number of parameters optimised in the inverse procedure reduced the uncertainty of the fitted parameters without significantly affecting the accuracy of model predictions. Further, the *Fit All* scenario gave high correlations of three parameters in comparison to the one high value for the *Set Measured* scenario ([Table 3](#)). Limiting the number of parameters in the inverse scenario was shown to be advantageous because parameter variation was reduced. These findings are consistent with the recommendations of [Hopmans et al. \(2002\)](#) but contrast with the study of [Sonnleitner, Abbaspour & Schulin \(2003\)](#). The latter work indicated that maximising the number of variables in the inverse optimisation increased the ability of parameters to describe water flow in alternative scenarios.

In our wedge study, only minor differences were observed between predictions when the number of optimised parameters was reduced. Furthermore, reducing the number of parameters in the inverse optimisation was advantageous because parameter uncertainty was reduced ([Table 2](#)). Our results show that, where practical, there is benefit in conducting additional measurements to estimate  $\theta_s$  and  $K_{\text{sat}}$ , which are two of the most sensitive parameters of the model ([Arbat et al., 2008](#)). The benefits of using measured

parameters, in combination with inverse modelling of water content data, has also been demonstrated by [Kandelous et al. \(2011\)](#). In these columns, hydraulic conductivity is not independently measured; rather sorptivity is measured and the hydraulic conductivity must be inferred with a model.

Including solute reaction parameters enables the Hydrus model to accurately predict reactive solute distribution in the soil. The retardation in the  $\text{NO}_3^-$  relative to the inflowing water indicates that the solute was adsorbed by the soil. Sorption of  $\text{NO}_3^-$  was included in Hydrus by using the Langmuir equation to approximate the partitioning of  $\text{NO}_3^-$  between the soil solution and the adsorbed phases. The Langmuir equation has been used previously to describe solute adsorption in soil ([Katou, Clothier & Green, 1996](#); [Qafoku, Sumner & Radcliffe, 2000](#); [Phillips, 2006](#)).

The distribution of solutes adsorbed to soil during water flow has been simulated under point-source infiltration in previous studies using Hydrus 2D/3D ([Hanson, Šimůnek & Hopmans, 2006](#)). However, validation under these flow scenarios has received little attention. [Ben-Gal & Dudley \(2003\)](#) observed that predictions of reactive P transport from a drip irrigation system showed a similar distribution to measured data, but they did not make any statistical comparisons. Reactive solute transport was previously validated under other flow scenarios ([Persicani, 1995](#); [Moradi, Abbaspour & Afyuni, 2005](#)). Our results validate the inclusion of the Langmuir equation in Hydrus for the prediction of reactive solute movement for 1D and 3D flow conditions. Furthermore, the results show that reactive solute parameters determined from relatively simple 1D adsorption columns can be used to accurately predict solute distribution under 3D conditions.

Other studies that have used Hydrus to predict water movement through soils have utilised PTFs to estimate soil hydraulic parameters ([Epino et al., 1996](#); [Skaggs et al., 2004](#); [Li, Zhang & Rao, 2005](#); [Phillips, 2006](#); [Siyal & Skaggs, 2009](#)). The suitability of parameters predicted by PTFs relies on the amount of data collected from soils with similar particle size distribution, bulk density, and water-holding capacity. We investigated use of the Rosetta model ([Schaap, Leij & Van Genuchten, 2001](#)) to obtain parameters for the same Red Ferrosol used here, but it provided less accurate estimates of water distribution in comparison to parameters determined from inverse modelling ([Fig. 4](#)). The high value of the pore connectivity parameter,  $l$  ([Table 2](#)), that resulted from inverse optimisation is in contrast to the value of 0.5 used on the Rosetta model ([Cook & Cresswell, 2007](#)). This difference may explain the limitations of Rosetta to accurately predict water flow in the repacked columns in these particular experiments.

This finding contrasts with those of [Kandelous & Šimůnek \(2010a\)](#) where parameters estimated from Rosetta produced acceptable predictions of water movement in laboratory studies. The differing results in our study may be in part due to the limited data for Australian Red Ferrosols available in the Rosetta soil database. In general, this paper confirms that inverse optimisation is advantageous provided enough data has been collected over a sufficient range of water contents ([Šimůnek et al., 2000](#); [Sonnleitner, Abbaspour & Schulin, 2003](#)). The use of inverse optimisation applied to horizontal infiltration columns provides a simple technique to accurately determine reaction parameters.

If parameters determined from inverse optimisation are to successfully describe water flow in alternative scenarios the soil properties must be the same. This was achieved in our laboratory because careful packing was possible in both the horizontal columns and soil wedges. For a field scenario, a similar method of predicting water and solute flow would need laboratory experiments on undisturbed cores. Similarly, *Kandelous & Šimůnek (2010a)* found that parameters suitable for describing water movement in packed laboratory columns were not capable of describing water distribution in an undisturbed field soil.

## CONCLUSION

Inverse modelling procedures in Hydrus confirm that soil hydraulic parameters can be reliably obtained from simple 1D diffusive water uptake soil column studies. The derived parameters are capable of accurately describing diffusive water movement over extended times and in alternative dynamic flow scenarios to those in which they were fitted. These results demonstrate that simple water uptake column experiments can be used to provide suitable flow conditions for accurate determination of reaction parameters under dynamic flow conditions. Reducing the number of parameters in the optimisation procedures by imposing independently measured values for  $\theta_s$ ,  $\theta_r$ , and  $K_{sat}$  decreased parameter uncertainty (or increased parameter uniqueness) without significantly impacting the accuracy of model predictions. These results show there is merit in pursuing this method in more complex scenarios since it may provide a simpler and cheaper way of determining hydraulic parameters in field conditions.

Solution  $\text{NO}_3^-$  and adsorbed  $\text{NO}_3^-$  concentrations collected from a combined water uptake- $\text{NO}_3^-$  tracer test provided the data to fit the reaction parameters for the Langmuir isotherm, which in turn were included in the Hydrus model to predict reactive solute transport. We have demonstrated the ability of HYDRUS to integrate unsaturated flow processes and independently determined reactive transport processes based on independent experiments involving the complex interplay of dynamic flow and reactive transport.

## ACKNOWLEDGEMENTS

We thank Dr Freeman Cook for his assistance with Hydrus modelling and Dr David Smiles for providing his expertise in experimental design and analysis.

## ADDITIONAL INFORMATION AND DECLARATIONS

### Funding

An Australian Federal Government Postgraduate Scholarship supported Dr. Kirkam's research. The funders had no role in study design, data collection and analysis, decision to publish, or preparation of the manuscript.

### Grant Disclosure

The following grant information was disclosed by the authors:  
Australian Federal Government Postgraduate Scholarship.

## Competing Interests

The authors declare that they have no competing interests.

## Author Contributions

- James M. Kirkham conceived and designed the experiments, performed the experiments, analyzed the data, contributed reagents/materials/analysis tools, prepared figures and/or tables, authored or reviewed drafts of the paper, approved the final draft.
- Christopher J. Smith conceived and designed the experiments, analyzed the data, contributed reagents/materials/analysis tools, authored or reviewed drafts of the paper, approved the final draft.
- Richard B. Doyle conceived and designed the experiments, authored or reviewed drafts of the paper, approved the final draft.
- Philip H. Brown conceived and designed the experiments, authored or reviewed drafts of the paper, approved the final draft.

## Data Availability

The following information was supplied regarding data availability:

Raw data is available as [Supplemental Files](#).

## Supplemental Information

Supplemental information for this article can be found online at <http://dx.doi.org/10.7717/peerj.6002#supplemental-information>.

## REFERENCES

- Ajdary K, Singh DK, Manoj Singh AK, Khanna M. 2007. Modelling of nitrogen leaching from experimental onion field under drip fertigation. *Agricultural Water Management* 89(1–2):15–28 DOI 10.1016/j.agwat.2006.12.014.
- Alpkem. 1992. *The flow solution*. Wilsonville: Alpkem Corporation.
- Arbat G, Puig-Bargues J, Bonany J, Barragan J, Ramirez De Cartagena F. 2008. Monitoring soil water status for micro-irrigation management versus modelling approach. *Biosystems Engineering* 100(2):286–296 DOI 10.1016/j.biosystemseng.2008.02.008.
- Ben-Gal A, Dudley LM. 2003. Phosphorus availability under continuous point source irrigation. *Soil Science Society of America Journal* 67(5):1449–1456 DOI 10.2136/sssaj2003.1449.
- Cook FJ, Cresswell HP. 2007. Estimation of soil hydraulic properties. In: Carter MR, Gregorich EG, eds. *Soil sampling and methods of analysis, canadian society of soil science*. Boca Raton: Taylor and Francis, LLC, 1139–1161.
- Cook FJ, Thorburn PJ, Fitch P, Bristow KL. 2003. WetUp: a software tool to display approximate wetting patterns from drippers. *Irrigation Science* 22(3–4):129–134 DOI 10.1007/s00271-003-0078-2.
- Cote CM, Bristow P, Charlesworth PB, Cook FJ, Thorburn PJ. 2003. Analysis of soil wetting and solute transport in subsurface trickle irrigation. *Irrigation Science* 22(3–4):143–156 DOI 10.1007/s00271-003-0080-8.
- Cresswell HP. 2002. The soil water characteristic. In: McKenzie N, Coughlan K, Cresswell HP, eds. *soil physical measurement and interpretation for land evaluation*. Collingwood: CSIRO Publishing, 59–84.

- Epino A, Mallants D, Vanclooster M, Feyen J. 1996. Cautionary notes on the use of pedotransfer functions for estimating soil hydraulic properties. *Agricultural Water Management* 29(3):235–253 DOI 10.1016/0378-3774(95)01210-9.
- Gardenas AI, Hopmans JW, Hanson BR, Šimůnek J. 2005. Two-dimensional modeling of nitrate leaching for various fertigation scenarios under micro-irrigation. *Agricultural Water Management* 74(3):219–242 DOI 10.1016/j.agwat.2004.11.011.
- Gee GW, Bauder JW. 1986. Particle-size analysis. In: Klute A, ed. *Methods of soil analysis. Part 1. Physical and mineralogical methods*. Madison: ASA and SSSA, 383–411.
- Hanson BR, Šimůnek J, Hopmans JW. 2006. Evaluation of urea–ammonium–nitrate fertigation with drip irrigation using numerical modeling. *Agricultural Water Management* 86(1–2):102–113 DOI 10.1016/j.agwat.2006.06.013.
- Hopmans JW, Šimůnek J, Romano N, Durner W. 2002. Inverse methods. In: Dane JH, Topp GC, eds. *Methods of soil analysis. Part 4. Physical methods Chapter*. Vol. 3. Madison: SSSA, 963–1008.
- Isbell RF. 1996. *The Australian soil classification*. Collingwood: CSIRO Publishing.
- Kandelous MM, Šimůnek J. 2010a. Comparison of numerical, analytical and empirical models to estimate wetting pattern for surface and subsurface drip irrigation. *Irrigation Science* 28(5):435–444 DOI 10.1007/s00271-009-0205-9.
- Kandelous MM, Šimůnek J. 2010b. Numerical simulations of water movement in a subsurface drip irrigation system under field and laboratory conditions using HYDRUS-2D. *Agricultural Water Management* 97(7):1070–1076 DOI 10.1016/j.agwat.2010.02.012.
- Kandelous MM, Šimůnek J, Van Genuchten MT, Malek K. 2011. Soil water content distributions between two emitters of a subsurface drip irrigation system. *Soil Science Society of America Journal* 75(2):488–497 DOI 10.2136/sssaj2010.0181.
- Katou H, Clothier BE, Green SR. 1996. Anion transport involving competitive adsorption during transient water flow in an Andisol. *Soil Science Society of America Journal* 60(5):1368–1375 DOI 10.2136/sssaj1996.03615995006000050011x.
- Kuntz D, Grathwohl P. 2009. Comparison of steady-state and transient flow conditions on reactive transport of contaminants in the vadose soil zone. *Journal of Hydrology* 369(3–4):225–233 DOI 10.1016/j.jhydrol.2009.02.006.
- Li J, Zhang J, Rao M. 2005. Modeling of water flow and nitrate transport under surface drip fertigation. *Transactions of the ASAE* 48(2):627–637 DOI 10.13031/2013.18336.
- Li J, Zhang J, Ren J. 2003. Water and nitrogen distribution as affected by fertigation of ammonium nitrate from a point source. *Irrigation Science* 22(1):19–30.
- Mallants D, Antonov D, Karastanev D, Perko J. 2007. Innovative in-situ determination of unsaturated hydraulic properties in deep Loess sediments in North-West Bulgaria. In: *Proceedings of the 11th International Conference on Environmental Remediation and Radioactive Waste Management (ICEM07-7202)*, Bruges, 1–7.
- McKenzie N, Coughlan K, Cresswell H. 2002. *Soil physical measurement and interpretation for land evaluation*. Melbourne: CSIRO.
- Molinero J, Raposo JR, Galindez JM, Arcos D, Guimera J. 2008. Coupled hydrogeological and reactive transport modelling of the Simpevarp area (Sweden). *Applied Geochemistry* 23(7):1957–1981 DOI 10.1016/j.apgeochem.2008.02.020.
- Moradi A, Abbaspour KC, Afyuni M. 2005. Modelling field-scale cadmium transport below the root zone of a sewage sludge amended soil in an arid region in Central Iran. *Journal of Contaminant Hydrology* 79(3–4):187–206 DOI 10.1016/j.jconhyd.2005.07.005.



- Nakagawa K, Hosokawa T, Wada SI, Momii K, Jinno K, Berndtsson R. 2010. Modelling reactive solute transport from groundwater to soil surface under evaporation. *Hydrological Processes* 24(5):608–617 DOI 10.1002/hyp.7555.
- Patel N, Rajput TBS. 2008. Dynamics and modeling of soil water under subsurface drip irrigated onion. *Agricultural Water Management* 95(12):1335–1349 DOI 10.1016/j.agwat.2008.06.002.
- Persicani D. 1995. Analysis of leaching behaviour of sludge-applied metals in two field soils. *Water, Air, & Soil Pollution* 83(1–2):1–20 DOI 10.1007/BF00482590.
- Phillips IR. 2006. Modelling water and chemical transport in large undisturbed soil cores using HYDRUS-2D. *Australian Journal of Soil Research* 44(1):27–34 DOI 10.1071/SR05109.
- Phillips IR, Bond WJ. 1989. Extraction procedure for determining solution and exchangeable ions on the same soil sample. *Soil Science Society of America Journal* 53(4):1294–1297 DOI 10.2136/sssaj1989.03615995005300040050x.
- Qafoku NP, Sumner ME, Radcliffe DE. 2000. Anion transport in columns of variable charge subsoils: nitrate and chloride. *Journal of Environmental Quality* 29(2):484–493 DOI 10.2134/jeq2000.00472425002900020017x.
- Rassam DW, Cook FJ. 2002. Numerical simulations of water flow and solute transport applied to acid sulphate soils. *Journal of Irrigation and Drainage Engineering* 128(2):107–115 DOI 10.1061/(ASCE)0733-9437(2002)128:2(107).
- Rassam DW, Cook FJ, Gardner EA. 2002. Field and laboratory studies of acid sulphate soils. *Journal of Irrigation and Drainage Engineering* 128(2):100–106 DOI 10.1061/(ASCE)0733-9437(2002)128:2(100).
- Rayment GE, Higginson FR. 1992. *Australian laboratory handbook of soil and water chemical methods*. Melbourne: Inkata Press.
- Reynolds WD, Elrick DE, Youngs EG, Amoozegar A, Booltink HWG, Bouma J. 2002. Saturated and field-saturated water flow parameters. In: Dane JH, Topp GC, eds. *Methods of soil analysis. Part 4. Physical methods*. Madison: SSSA, 797–878.
- Ramos TB, Simunek J, Goncalves MC, Martins JC, Prazeres A, Castanheira NL, Pereira LS. 2011. Field evaluation of a multicomponent solute transport model in soils irrigated with saline waters. *Journal of Hydrology* 407(1–4):129–144 DOI 10.1016/j.jhydrol.2011.07.016.
- Ramos TB, Simunek J, Goncalves MC, Martins JC, Prazeres A, Pereira LS. 2012. Two-dimensional modeling of water and nitrogen fate from sweet sorghum irrigated with fresh and blended saline waters. *Journal of Hydrology* 111:87–104 DOI 10.1016/j.agwat.2012.05.007.
- Schaap MG, Leij FJ, Van Genuchten MT. 2001. Rosetta: a computer program for estimating soil hydraulic parameters with hierarchical pedotransfer functions. *Journal of Hydrology* 251(3–4):163–176 DOI 10.1016/S0022-1694(01)00466-8.
- Šimůnek J, Hopmans JW, Nielsen DR, Van Genuchten MT. 2000. Horizontal infiltration revisited using parameter estimation. *Soil Science* 165(9):708–717 DOI 10.1097/00010694-200009000-00004.
- Šimůnek J, Šejna M, Saito H, Sakai M, Van Genuchten MT. 2008. *The HYDRUS-1D software package for simulating the movement of water, heat, and multiple solutes in variably saturated media, Version 4.0, HYDRUS Software Series 3*. Riverside: Department of Environmental Sciences, University of California Riverside, 315. Available at [https://www.pc-progress.com/Downloads/Pgm\\_hydrus1D/HYDRUS1D-4.08.pdf](https://www.pc-progress.com/Downloads/Pgm_hydrus1D/HYDRUS1D-4.08.pdf).
- Šimůnek J, Van Genuchten MT. 1996. Estimating unsaturated soil hydraulic properties from tension disc infiltrometer data by numerical inversion. *Water Resources Research* 32:2683–2696.
- Šimůnek J, Van Genuchten MT, Šejna M. 2006. *The HYDRUS software package for simulating two- and three-dimensional movement of water, heat, and multiple solutes in variably-saturated media*.



- Technical manual. Version 1.0.* Prague: PC Progress, 241. Available at [https://www.pc-progress.com/downloads/Pgm\\_Hydrus3D/HYDRUS3D%20Technical%20Manual.pdf](https://www.pc-progress.com/downloads/Pgm_Hydrus3D/HYDRUS3D%20Technical%20Manual.pdf).
- Siyal AA, Skaggs TH. 2009.** Measured and simulated soil wetting patterns under porous clay pipe sub-surface irrigation. *Agricultural Water Management* **96**(6):893–904 DOI [10.1016/j.agwat.2008.11.013](https://doi.org/10.1016/j.agwat.2008.11.013).
- Skaggs TH, Trout TJ, Šimůnek J, Shouse PJ. 2004.** Comparison of HYDRUS-2D simulations of drip irrigation with experimental observations. *Journal of Irrigation and Drainage Engineering* **130**(4):304–310 DOI [10.1061/\(ASCE\)0733-9437\(2004\)130:4\(304\)](https://doi.org/10.1061/(ASCE)0733-9437(2004)130:4(304)).
- Smiles DE, Philip JR, Knight JH, Elrick DE. 1978.** Hydrodynamic dispersion during absorption of water by soil. *Soil Science Society of America Journal* **42**(2):229–234 DOI [10.2136/sssaj1978.03615995004200020002x](https://doi.org/10.2136/sssaj1978.03615995004200020002x).
- Sonnleitner MA, Abbaspour KC, Schulin R. 2003.** Hydraulic and transport properties of the plant-soil system estimated by inverse modelling. *European Journal of Soil Science* **54**(1):127–138 DOI [10.1046/j.1365-2389.2002.00491.x](https://doi.org/10.1046/j.1365-2389.2002.00491.x).
- Sposito G. 1989.** *The chemistry of soils*. New York: Oxford University Press.
- Van Dam JC, Stricker JNM, Droogers P. 1994.** Inverse method to determine soil hydraulic functions from multistep outflow experiments. *Soil Science Society of America Journal* **58**(3):647–652 DOI [10.2136/sssaj1994.03615995005800030002x](https://doi.org/10.2136/sssaj1994.03615995005800030002x).
- Vrugt JA, Bouten W. 2002.** Validity of first order approximations to describe parameter uncertainty in soil hydrological models. *Soil Science Society of America Journal* **66**(6):1740–1751 DOI [10.2136/sssaj2002.1740](https://doi.org/10.2136/sssaj2002.1740).
- Wagenet RJ, Hutson JL. 1989.** *LEACHM: Leaching estimation and solute movement – a processed based model of water and solute movement, transformations, plant uptake and chemical reactions in the unsaturated zone*. Continuum Vol. 2. Ithica: Water Resources Institute, Cornell University.
- Walkley A, Black IA. 1934.** An examination of the Degtjareff method for determining soil organic matter and a proposed modification of the chromic acid titration method. *Soil Science* **37**(1):29–38 DOI [10.1097/00010694-193401000-00003](https://doi.org/10.1097/00010694-193401000-00003).
- Wöhling T, Vrugt JA, Barkle GF. 2008.** Comparison of three multiobjective optimization algorithms for inverse modeling of vadose zone hydraulic properties. *Soil Science Society of America Journal* **72**(2):305–319 DOI [10.2136/sssaj2007.0176](https://doi.org/10.2136/sssaj2007.0176).
- Wu G, Chieng ST. 1995a.** Modeling multicomponent reactive chemical transport in nonisothermal unsaturated/saturated soils. Part 1. Mathematical model development. *Transactions of the ASAE* **38**(3):817–826 DOI [10.13031/2013.27896](https://doi.org/10.13031/2013.27896).
- Wu G, Chieng ST. 1995b.** Modeling multicomponent reactive chemical transport in nonisothermal unsaturated/saturated soils. Part 2. Numerical simulations. *Transactions of the ASAE* **38**(3):827–838 DOI [10.13031/2013.27897](https://doi.org/10.13031/2013.27897).